Manickam-Periyaraman, P.; Espinosa, JC.; Ferrer Ribera, RB.; Subramanian, S.; Alvaro Rodríguez, MM.; García Gómez, H.; Navalón Oltra, S. (2020). Bimetallic iron-copper oxide nanoparticles supported on nanometric diamond as efficient and stable sunlight-assisted Fenton photocatalyst. Chemical Engineering Journal. 393:1-11. https://doi.org/10.1016/j.cej.2020.124770

Bimetallic iron-copper oxide nanoparticles supported on nanometric diamond as efficient and stable sunlight-assisted Fenton photocatalyst

Premkumar Manickam-Periyaraman,[1,&] Juan C. Espinosa,[2,&] Belén Ferrer,[2] S. Sivanesan,[1] Mercedes Álvaro,[2] Hermenegildo García,[2,3,*] Sergio Navalón[2,*]

hgarcia@qim.upv.es; sernaol@doctor.upv.es

[1] Department of Applied Science and Technology, Anna University, Sardar Patel Road, 600025, Chennai, India

[2] Departamento de Química and Instituto de Tecnología Química CSIC-UPV, Universitat Politècnica de València, Consejo Superior de Investigaciones Científicas, Av. de los Naranjos s/n, 46022, Valencia, Spain

[3] Center of Excellence for Advanced Materials Research, King Abdulaziz University, Jeddah, Saudi Arabia

Abstract

Bimetallic iron and copper oxide nanoparticles (NPs) supported on hydroxylated diamond (D3) exhibits an improved activity for the heterogeneous Fenton phenol degradation under natural or simulated sunlight irradiation with respect to analogous monometallic samples or than analogous FeCu NPs on graphite, activated carbon and P25 TiO_2 semiconductor. FeCu/D3 catalyst exhibits good recyclability and stability especially working at pH 6. Overall, the high activity of the $Fe_{20}Cu_{80}$(0.2 wt%)/D3 catalyst is mainly due to the combination of the high activity of reduced copper species decomposing H_2O_2 to $HO^{\cdot}$ radical, while Fe^{2+} allows the regeneration of these reduced copper species.

Keywords: (photo)Fenton reaction; heterogeneous catalysis; FeCu bimetallic nanoparticles; diamond nanoparticles; natural sunlight irradiation.

[&] both are considered first authors

1. Introduction

Advanced oxidation processes (AOPs) are chemical processes having in common the generation of highly aggressive radicals, such as hydroxyl radicals, to trigger the oxidative decomposition of chemicals and pollutants [1-4]. The high oxidation potential of hydroxyl radicals makes AOPs treatments of general applicability for the treatment of toxic, non-biodegradable and/or recalcitrant organic pollutants in water, soil and air [5-8]. Among the different AOPs, the homogeneous (photo)Fenton reaction has attracted over the years a continuous interest for water remediation due to its efficiency and easy implementation at industrial scale (Equations 1 and 2) [9-11]. The main drawbacks, however, associated to the homogeneous (photo)Fenton reaction that limit its application include [9-11]: i) the need of acid pH values to have photocatalytically active iron species such as $Fe(OH)^{2+}$; ii) the need to remove dissolved iron salts at the end of the treatment to meet water regulations (Fe content <2 mg L^{-1}) with the subsequent sludge formation; and iii) the need to employ artificial UV light (~300 nm) to excite the Fe^{3+} species (Equation 2).

$$Fe^{2+} + H_2O_2 \xrightarrow[pH \sim 3]{} Fe^{3+} + HO^{\cdot} + HO^{-} \quad \text{(Equation 1)}$$

$$Fe(OH)^{2+} \xrightarrow[pH \sim 3]{UV\text{-}Vis} Fe^{2+} + HO^{\cdot} \quad \text{(Equation 2)}$$

Fortunately, heterogeneous (photo)Fenton catalysts can ameliorate the problems associated with the homogeneous ones [12, 13]. Some of the most active (photo)Fenton materials are based on noble or transition metal NPs supported in high surface area supports such as metal oxides [13], aluminosilicates [6] or carbonaceous materials [14]. Among them, Au [15] or Ag [16] NPs supported on the hydroxylated surface of diamond NPs (D) have resulted among the most efficient and stable photocatalysts developed for visible light irradiation using phenol as model pollutant. Analogous Cu NPs supported on nanometric D

become deactivated due to the oxidation of the catalytically active reduced Cu species to Cu^{2+} [17]. Recently, iron oxide NPs supported on the surface of hydroxylated D NPs (Fe_{ox}/D) has exhibited photocatalytic activity and stability for the visible light assisted Fenton reaction even working at pH values around 6 [18]. Importantly, these works have demonstrated the superiority of D NPs as support over other alternative solids as activated carbon, graphite, carbon nanotubes and even the benchmark semiconductor TiO_2 [16-18]. In general, the superior activity of the metal NPs supported on D NPs has been attributed to the combination of a good dispersion and small size of supported metal NPs, together with the inertness of the diamond surface allowing $HO^{\cdot}$ radicals to diffuse freely into the aqueous solution.

In this work, the catalytic activity of bimetallic Fe_xCu_y oxide NPs supported on several carbonaceous materials with enhanced activity for the heterogeneous (photo)Fenton reaction assisted by natural or simulated sunlight irradiation is reported. The superior activity of $Fe_{20}Cu_{80}$ at 0.2 wt% supported onto the hydroxylated surface of nanodiamonds (D3) will be justified as derived from the combination of the high rate constant for hydroxyl radical formation of Cu^{+} species and the presence of the optimal Fe^{2+} concentration to efficiently restore oxidized Cu^{2+} to the catalytically active Cu^{+} oxidation state.

2. Experimental section

The list of materials used in the present study is indicated in the supporting information (Section S1). Catalyst preparation is described in detail in supporting information sections S2-S3. Briefly, the mono- or bimetallic catalysts were prepared by deposition of the corresponding metal NPs (Fe, Cu or FeCu) onto the surface of commercial carbonaceous supports (diamond NPs, D; graphite, G; or activated carbon, AC) modified or not by chemical and thermal treatments as previously reported [15]. These carbonaceous supports are from the same batch than those previously reported [16-18]. The chemical treatment of the commercial carbonaceous supports (D1, G1 or AC1) by homogeneous Fenton reaction leads to the formation of the carbonaceous supports labelled as D2, G2 or AC2. The conditions of the Fenton reaction are indicated in the supporting information (Section S2). The Fenton-treated carbon supports (D2, G2 or AC2) were further annealed under H_2 at 500 ºC (Section 2).

Supporting information (Sections S4, S5 and S6) lists the techniques and procedures followed to characterize the materials. The course of phenol degradation was followed as indicated in the supporting information Section S4. Photocatalytic experiments are described in section S7.

3. Results and discussion

3.1. Catalyst preparation and characterization

Commercial D NPs, G and AC were submitted to an oxidative homogeneous Fenton treatment followed or not by thermal annealing under hydrogen atmosphere at 500 ºC (Section S2). This procedure has been previously reported to remove impurities from the sample surface introducing surface oxygen functional groups, where subsequently small

metal nanoparticles (MNPs) can be grafted [15]. In general, the homogeneous Fenton treatment of the carbonaceous samples generates hydroxyls, carbonyls and carboxylic groups on the surface. The hydrogen annealing of the Fenton-treated samples results in the chemical reduction of oxygenated functional groups, causing the prevalence of surface hydroxyl groups [15].

In a subsequent stage, mono- and bimetallic M NPs of iron and/or copper were deposited at 0.2 wt% loading on the parent or modified carbonaceous samples (D1-3, G1-3 or AC1-3) using the well-known polyol method (Section S3) [16-18]. This method consists in the chemical reduction of metal salts to MNPs by heating a suspension of the carbonaceous material in ethylene glycol. For comparison, the most active MNPs tested in this work having $Fe_{20}Cu_{80}$ proportions were also deposited on TiO_2 as the benchmark photocatalyst. Table 1 lists the series of catalysts employed in the present work, the average particle size distribution and standard deviation estimated from TEM images (Figure 1 and Figures S2-S7) as well as some relevant catalytic data.

In order to get more insights about the spontaneous oxidation of bimetallic FeCu NPs under ambient conditions, unsupported $Fe_{20}Cu_{80}$ NPs were also prepared by chemical reduction of a mixture of Fe^{2+} and Cu^{2+} by $NaBH_4$ (Section S3). Supporting information contains an extensive characterization of this unsupported $Fe_{20}Cu_{80}$ sample.

The presence of supported bimetallic FeCu NPs was assessed by EDX analysis of the samples during TEM measurements (Figure 1). BF-SEM measurements of the bimetallic NP supported on the carbon materials under study were also performed to characterize the MNP morphology as well as further confirm the M NP particle size (Figures S8-S18). Regardless the metal composition or the carbon support employed to deposit the bimetallic NPs a non-

homogeneous variety of cubic, polyhedral NPs as well as NPs lacking defined geometrical shape of different sizes were observed.

In order to get more insights about the composition of the most active sample prepared in this study $Fe_{20}Cu_{80}$(0.2wt%)/D3 additional BF-SEM coupled with EDX (BF-SEM/EDX) analysis and HR-TEM measurements were carried out. BF-SEM/EDX analysis of a MNP present in the $Fe_{20}Cu_{80}$(0.2wt%)/D3 sample measured across the NP (line scan) confirms the formation of Fe and Cu alloy NP by the coincidence of the profiles of the two elements (Figure S19). HR-TEM analysis of the $Fe_{20}Cu_{80}$(0.2wt%)/D3 also reveals the formation of alloyed NPs (Figure S20) with interplanar distances similar to that of Cu_{ox}(0.2wt%)/D3, a fact not unexpected in view of the larger proportion of Cu atoms (Figure S21).

Table 1. Summary of the catalysts employed in the present work with a metal loading of 0.2 wt% (entries 1-14) or 1 wt% (entries 15-17) and activity data for the heterogeneous Fenton degradation of phenol assisted by simulated sunlight irradiation.[a] For the sake of comparison the activity of the catalysts Cu_{ox}(0.2 wt%)/D3 and Fe_{ox}(0.2 wt%)/D3 previously reported have been also studied under the present reaction conditions.

Entry	Catalyst	Average MNP size and standard deviation (nm)	Initial reaction rate (mM h^{-1})	TOF (h^{-1})	Phenol conversion (%) at 2 h	Ref.
1[b]	Cu_{ox}/D3	3.7 ± 2.7	0.43	68	80	[17]
2	$Fe_{20}Cu_{80}$/D3	4.1 ± 0.77	0.64	99	100	This work
3	$Fe_{50}Cu_{50}$/D3	5.4 ± 0.83	0.32	47	45	This work
4	$Fe_{80}Cu_{20}$/D3	4.3 ± 0.78	0.53	76	96	This work
5[b]	Fe_{ox}/D3	2.2 ± 0.5	0.51	71	86	[18]
6	$Fe_{20}Cu_{80}$/D2	5.6± 0.84	0.20	31	30	This work
7	$Fe_{20}Cu_{80}$/D1	8.4±0.95	0.10	15	15	This work
8	$Fe_{20}Cu_{80}$/AC3	6.1 ± 1.03	0.16	25	45	This work

9	$Fe_{20}Cu_{80}$/AC2	7.3 ± 1.16	0.05	8	16	This work
10	$Fe_{20}Cu_{80}$/AC1	8.6 ± 1.25	0.03	4	6	This work
11	$Fe_{20}Cu_{80}$/G3	4.8 ± 1.0	0.36	56	74	This work
12	$Fe_{20}Cu_{80}$/G2	7.9 ± 1.6	0.21	33	40	This work
13	$Fe_{20}Cu_{80}$/G1	8.7 ± 1.9	0.05	8	11	This work
14	$Fe_{20}Cu_{80}/TiO_2$	1.4 ±0.20	0.51	80	81	This work
	TiO_2	-	0.38	-	35	
15	$Fe_{20}Cu_{80}$/D3	6.4 ± 1.02	0.64	20	100	This work
16 [b]	Fe_{ox}/D3	2.4 ± 0.40	0.43	13	85	[18]
17 [a]	Cu_{ox}/D3	11.1 ± 5.60	0.33	10	79	[17]

[a] Reaction conditions: catalyst (~200 mg/L, 0.0071 mM supported Cu and/or Fe), phenol (100 mg L^{-1}, 1.06 mM), H_2O_2 (200 mg L^{-1}; 5.88 mM), 20 ºC, pH 4**,** simulated sunlight (1 sun).

[b] These catalysts have been previously reported (see refs) and the present samples correspond to the same batches as in the reference work.

Among the different bimetallic NPs supported on the carbonaceous materials (Table 1, entries 1-13), the smallest bimetallic FeCu NPs, were obtained using D3 as support and a molar proportion of $Fe_{20}Cu_{80}$ (Table 1, entry 2) at 0.2 wt% loading. The use of commercial D NPs (D1) (Table 1, entry 7) or Fenton-treated D (D2) (Table 1, entry 6) resulted in supported bimetallic $Fe_{20}Cu_{80}$ NPs with higher average particle size compared to D3. As previously reported for monometallic Au, Ag, Cu or Fe NPs supported on D3, a Fenton-treated commercial D NPs (D1) followed by hydrogen annealing at high temperature is a convenient treatment to achieve surface functionalization of D NPs mainly with hydroxyl groups that are better suited to achieve MNPs of small size. A similar trend has been also observed when using G or AC supports, the smallest $Fe_{20}Cu_{80}$ bimetallic NPs being obtained when using G (Table 1, entries 11-13) or AC (Table 1, entries 8-10) submitted to Fenton treatment and subsequent hydrogen annealing (G3 or AC3).

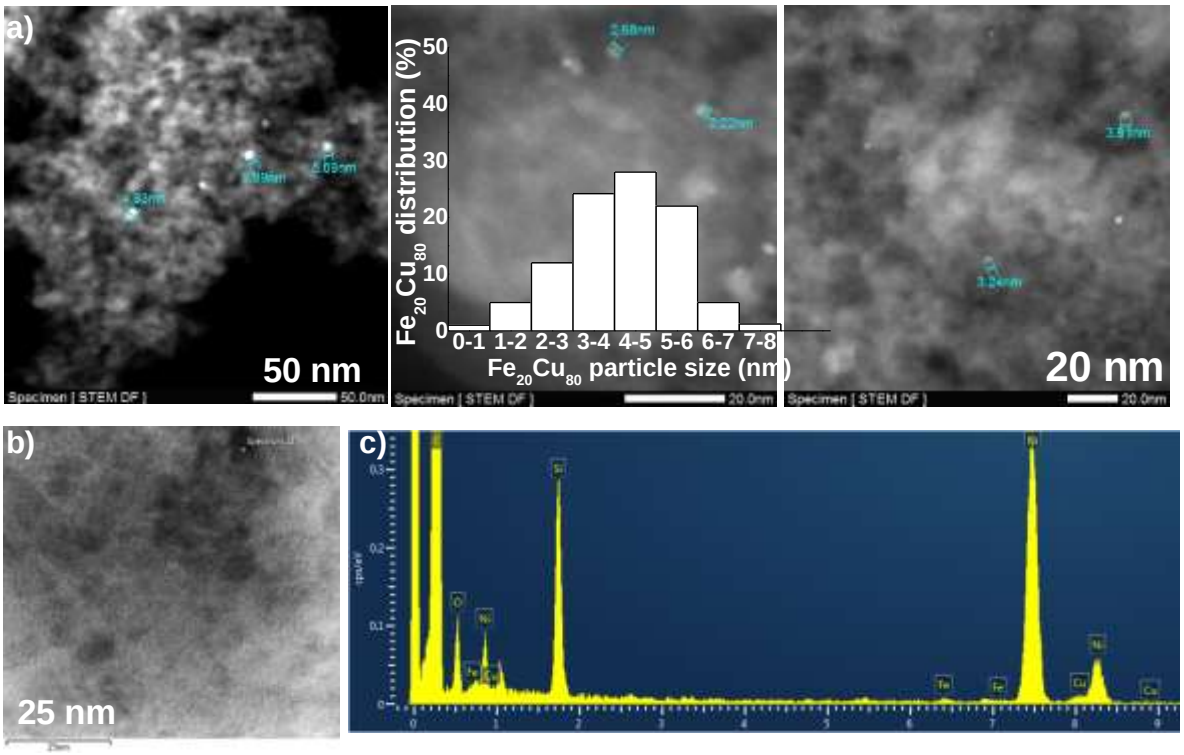

Figure 1. a) Dark-field-STEM images and MNP size distribution of $Fe_{20}Cu_{80}$/D3; b) Bright-field-STEM and, c) EDX spectrum of $Fe_{20}Cu_{80}$/D3. Metal loading 0.2 wt%. Nickel is present due to the TEM grid composition

Taking D3 as MNP support, it was observed that the Fe-Cu atomic proportion in the bimetallic NP influences somewhat the MNP size distribution (Table 1, entries 2-4). While using D3 as support, a molar ratio of $Fe_{20}Cu_{80}$ renders the smallest NPs (4.1 ± 0.77 nm), larger particle size were measured for $Fe_{50}Cu_{50}$ (5.4 ± 0.83 nm) supported on D3 at 0.2 wt%. In agreement with the expected behaviour, an increase of the metal loading from 0.2 to 1 w% for $Fe_{20}Cu_{80}$/D3 results in an increase of the MNP size (Table 1, entries 15-17 and Figure S6). Interestingly, an analogous catalyst using TiO_2 as support was prepared for bimetallic $Fe_{20}Cu_{80}$ MNP at 0.2 wt % loading (Table 1, entry 14), achieving in this case the smallest MNP size (1.4 ±0.20 nm).

PXRD measurements for bimetallic FeCu/D3 materials (Figure S22) did not allow the detection of any iron or copper species, probably due to the low metal loading (0.2 wt%) and the good dispersion of the small bimetallic MNPs as observed by TEM.[16-18, 21, 22]

XPS measurements of the $Fe_{20}Cu_{80}$/D3 sample at both metal loadings (0.2 and 1 wt%) shows the presence of weak and broad bands corresponding to these metals in their oxidized form (Figure 2). In the case of the $Fe_{20}Cu_{80}$/D3 samples at both 0.2 (Figure S23) or 1 wt% (Figure S24), the O 1s spectrum can be mainly fitted to two main peaks at 533.5 and 536.9 eV attributable to O atoms bonded to C by single bonds groups and carbonyl groups on the diamond surface, respectively. In the case of the $Fe_{20}Cu_{80}$(1 wt%)/D3 sample, the XPS deconvolution has allowed observing the presence of reduced Cu^0/Cu^+ and Fe^{2+}, together with the oxidized Cu^{2+} and Fe^{3+} species. Based on these XPS measurements and considering the behaviour of unsupported NPs (Figures S25-27), it is assumed that the bimetallic Fe_xCu_x NPs supported on D3 are in the form of oxides. This assumption was further supported by the EPR spectrum of the $Fe_{20}Cu_{80}$/D3 sample (see supporting information for the experimental details of EPR measurements) that shows a band centred at 3,365 G that can be attributed to the presence of Fe^{3+} and/or Cu^{2+} (see below Figure 7). It should be reminded that Fe^{2+}, Cu^+ and Cu^0 are EPR silent. Therefore, both EPR and XPS data indicate that at least the most external surface of the bimetallic FeCu NPs contain Fe^{3+} and Fe^{2+} together with Cu^{2+} and/or Cu^+/Cu^0 species.

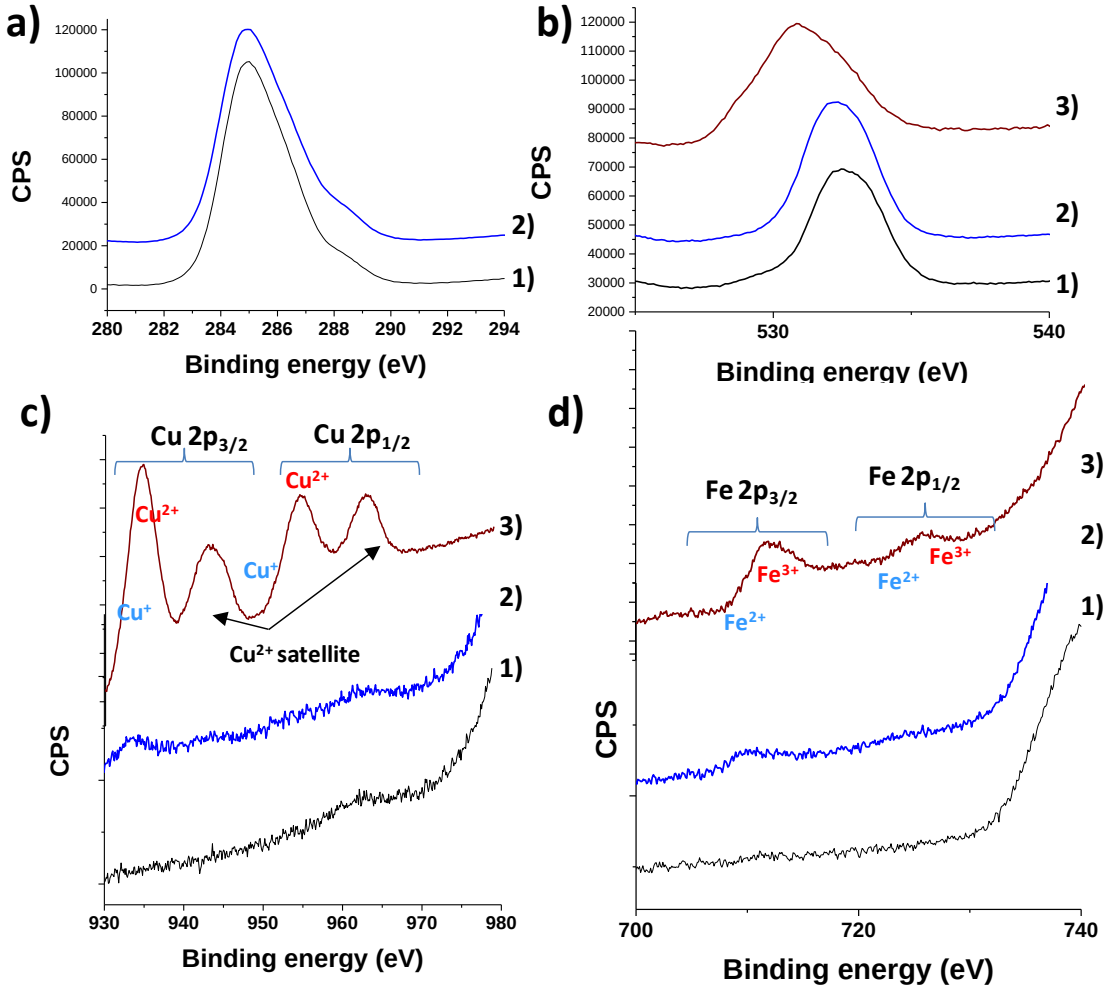

Figure 2. XPS of $Fe_{20}Cu_{80}$(0.2 wt%)/D3 (1), $Fe_{20}Cu_{80}$(1.0 wt%)/D3 (2) and unsupported $Fe_{20}Cu_{80}$ NPs (3). Legend: a) C1s, b) O1 s, c) Cu 2p and d) Fe 2p.

Furthermore, the interaction between the bimetallic NPs as a function of both the composition ($Fe_{80}Cu_{20}$/D3, $Fe_{50}Cu_{50}$/D3 and $Fe_{20}Cu_{80}$/D3) (Figure S24) and the carbon support ($Fe_{20}Cu_{80}$/D1, $Fe_{20}Cu_{80}$/D2, $Fe_{20}Cu_{80}$/AC3 and $Fe_{20}Cu_{80}$/G3) (Figures S28-S31) was studied by XPS measurements of the samples at 1 wt%. Table S1 summarizes the XPS data showing the atomic percentage (%) of copper and iron species present in the different catalysts under study based on XPS measurements.

From these XPS measurements it can be concluded that the higher the copper content in the bimetallic nanoparticle, the higher the proportion of Cu^{+} and Fe^{2+} that are the most

active species towards H_2O_2 reaction. In addition, the D3 support offers a relative stronger interaction with the metal nanoparticles respect to the use of non-functionalized D3 support. A more detailed explanation about the XPS measurements can be found in the supplementary information (section S7).

3.2. Catalytic activity

The activity as Fenton catalysts of the materials prepared in this work was tested for phenol degradation assisted by natural or simulated sunlight irradiation. Phenol was selected as model organic pollutant due to its toxicity and lack of biodegradability in conventional biological aerobic treatments. Preliminary experiments showed that phenol adsorption or degradation using the carbonaceous supports in the absence of metal NPs working at pH 4 is lower than 3 %. Phenol degradation under dark or natural sunlight irradiation in the presence of H_2O_2 as oxidant at pH 4, but in the absence of catalyst, is lower than 2 %. The use of mono- or bimetallic MNPs supported on the different carbonaceous materials as catalysts under continuous simulated sunlight irradiation resulted in phenol degradation and H_2O_2 decomposition in a different extent (Table 1, Figure 3 and Figures S32-S33). Thus, these experiments prove that both catalyst and sunlight irradiation are necessary to achieve significant phenol degradation under the present conditions. The most active catalysts prepared in this work are those based on bimetallic $Fe_{20}Cu_{80}$ NPs supported on the various D samples (D1, D2 or D3) compared to analogous catalysts based on G (Table 1, entries 11-13) or AC (Table 1 entries 8-10). This fact can be attributed to the small MNP size for D-supports and, in particular, the D3 support respect to the other carbonaceous materials [16-18]. In addition, the inertness of the D surface should also play a role. This observation, i.e. higher activity of $Fe_{20}Cu_{80}$ NPs supported on D catalysts respect to G or AC (Figure S32), is similar to those previously reported for monometallic NPs of Ag [16], Cu [17] or Fe [18] metals supported on D. Interestingly, for the three carbonaceous supports under study namely D, G

or AC a homogeneous Fenton treatment followed by hydrogen annealing at high temperature (D3, G3 or AC3) increases the activity of the MNPs on the carbonaceous surface, respect to the use of the Fenton-treated samples (D2, G2 or AC2) or the parent carbonaceous supports (D1, G1 or AC1). This result could be probably due to the small size of MNPs with enhanced activity. The smaller MNPs size obtained when using D3, G3 or AC3 supports can be attributed to the increased population of hydroxyl groups able to stabilize small MNPs.

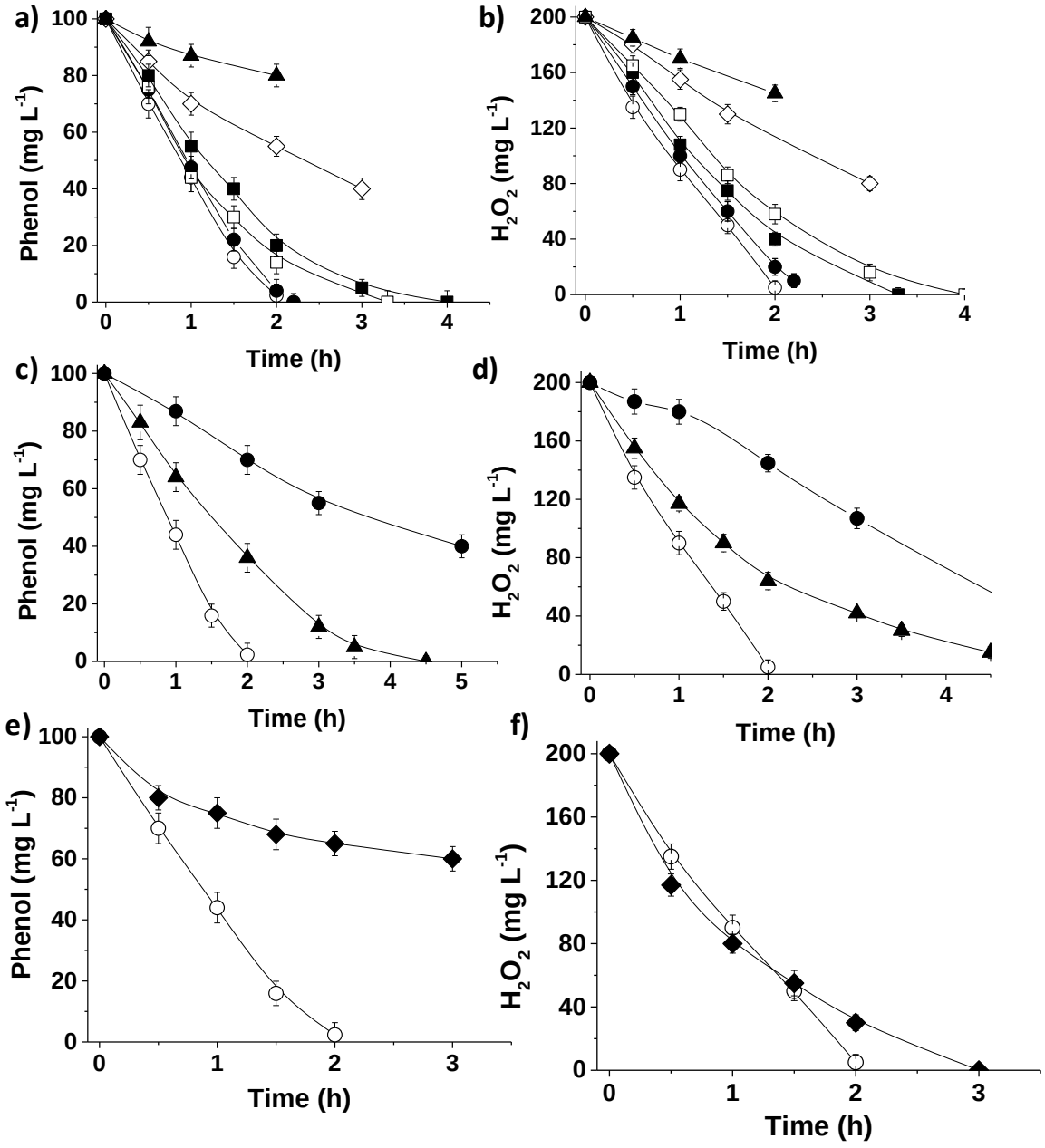

Figure 3. Phenol degradation (a,c and e) and H_2O_2 decomposition (b, d and f) using mono- and bimetallic oxidized NPs (0.2 wt%) supported on D3 under simulated sunlight irradiation at pH 4. Legend: (a, b) $Fe_{20}Cu_{80}$/D3 (○), $Fe_{80}Cu_{20}$/D3 (●), Fe_{ox}/D3 (□), Cu_{ox}/D3 (■), $Fe_{50}Cu_{50}$/D3 (◊). A control using $Fe_{20}Cu_{80}$/D3 (▲) under dark conditions is also shown. Legend (c, d): $Fe_{20}Cu_{80}$/D3 (○), $Fe_{20}Cu_{80}$/G3 (▲), $Fe_{20}Cu_{80}$/AC3 (●); Legend (e, f): $Fe_{20}Cu_{80}$/D3 (○), $Fe_{20}Cu_{80}$/TiO_2 (♦). Reaction conditions: Catalyst (~200 mg/L, 0.0071 mM supported Cu and/or Fe), phenol (100 mg L^{-1}, 1.06 mM), H_2O_2 (200 mg L^{-1}; 5.88 mM), 20 ºC, pH 4**,** simulated sunlight (1 sun).

Regardless the observation that the highest catalytic activity of bimetallic FeCu NPs supported on D3 correlates with the smaller metal NPs, there is an effect of the Fe to Cu proportion that will be discussed later in the reaction mechanism section. In fact, the catalytic activity of $Fe_{20}Cu_{80}$(0.2 wt%)/D3 is higher than that measured for monometallic Fe(0.2 wt%)/D3 or Cu(0.2 wt%)/D3 catalysts, even though its metal particle size is higher compared with that of monometallics (Table 1). This enhanced activity exemplifies the potential of tuning the composition of the MNPs to optimize the photocatalytic activity as it will be discussed later. Figure 4 also shows the remarkable enhancement of the catalytic activity when the reaction is carried out using $Fe_{20}Cu_{80}$(0.2 wt%)/D3 under simulated sunlight irradiation respect to dark conditions (Figure 3a-b).

The catalytic activity of the most active $Fe_{20}Cu_{80}$(0.2 wt%)/D3 sample is also higher than that of an analogous catalyst based of $Fe_{20}Cu_{80}$ NPs supported on TiO_2 considered as a benchmark photocatalyst TiO_2 (Figure 3). The lower activity of $Fe_{20}Cu_{80}$/TiO_2 can be explained considering the spurious decomposition of H_2O_2 by conduction band electron reduction to O_2 with minimum phenol degradation [18]. Previous studies reported by some of us have shown that, under similar reaction conditions, the use of TiO_2-P25 as catalysts leads

to H_2O_2 decomposition to molecular O_2 and probably also H_2O by disproportionation [17, 18].

In addition to the metallic catalyst composition, the metal loading of bimetallic $Fe_{20}Cu_{80}$/D3 (0.2 or 1wt%) also influences the resulting catalytic activity (Figure S33) probably due to the differences on the particle size distribution (Figure 1 and S7). The lower the metal loading (0.2 wt%), the lower the average MNP size and the higher the catalytic activity of $Fe_{20}Cu_{80}$/D3.

One of the challenges when developing heterogeneous catalysts for the (photo)Fenton is performing the reaction at neutral or even slightly basic pH conditions due to the shift in the decomposition mode of H_2O_2 from $HO^{\cdot}$ to $HOO^{\cdot}$ [23]. It should be noted that the homogeneous (photo)Fenton reaction is efficient under strongly acidic pH values (~3.5) in order to have the appropriate iron speciation. For the most active catalysts prepared in this work consisting in mono- or bimetallic FeCu NPs supported on D3, their (photo)catalytic activity under simulated sunlight irradiation was determined at different pH values (Figure 4). It was observed that regardless the pH value of the reaction medium, the most active catalyst was $Fe_{20}Cu_{80}$(0.2 wt%)/D3. As expected, the catalytic activity increased as the pH of the reaction medium decreases with the optimum at pH 4. Nevertheless, complete phenol degradation could be achieved even at pH 6 at sufficiently long reaction times. Importantly, it was observed that the difference in catalytic activity in favour of $Fe_{20}Cu_{80}$/D3 compared with monometallic catalysts increases as the pH of the solution increases, although monometallic Fe_{ox}(0.2 wt%)/D3 and Cu_{ox}(0.2 wt%)/D3 do not exhibit a linear correlation with the pH from 5 to 6, a fact that could be related to the shift in the H_2O_2 decomposition mechanism from hydroxyl to hydroperoxyl radical generation that occurs in the intermediate pH range [23]. This important observation highlights the potential of designing mixed metal oxides to

develop active and efficient heterogeneous (photo)Fenton catalysts able to operate at quasi neutral pH.

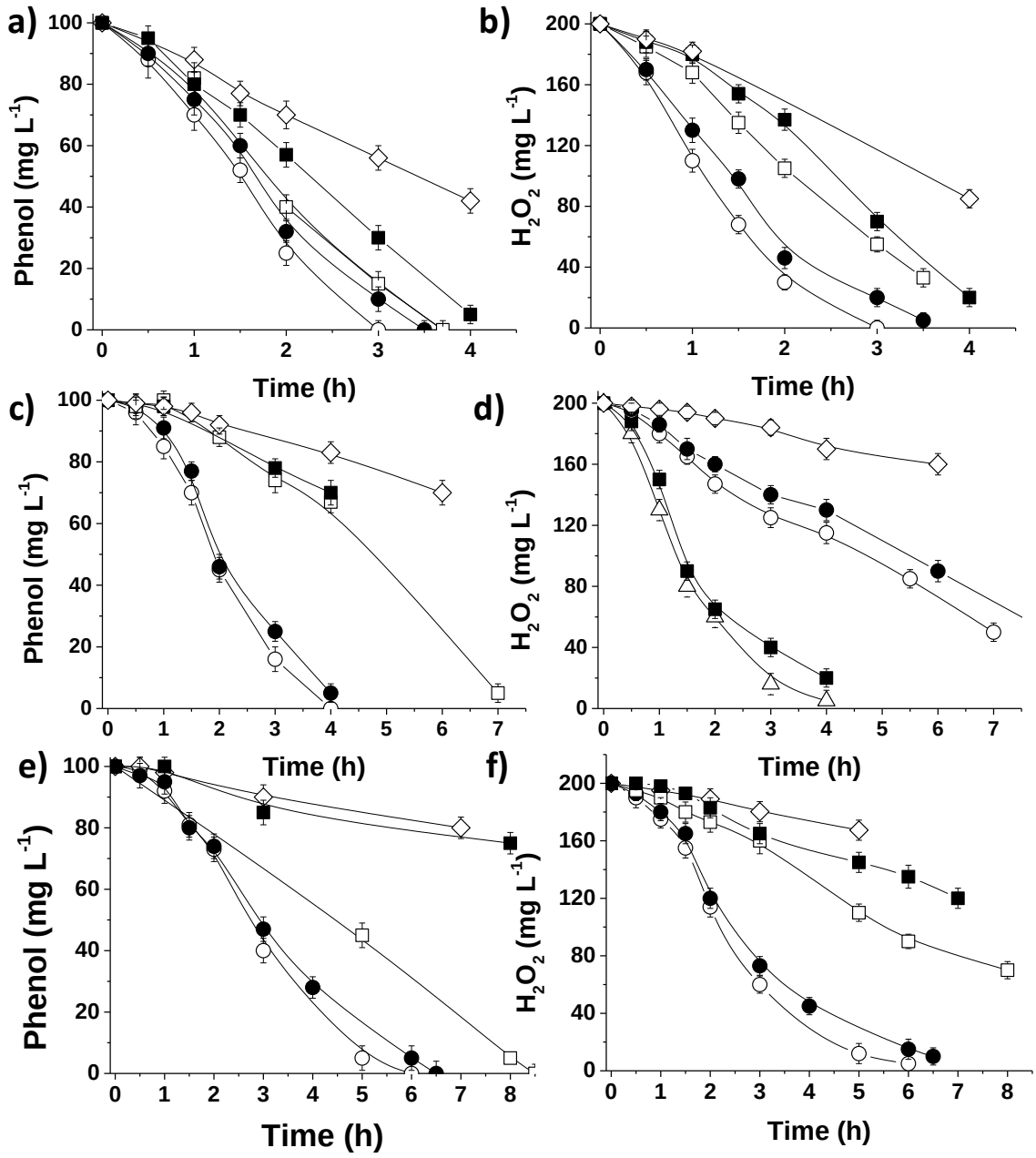

Figure 4. Phenol degradation (a, c and e) and H_2O_2 decomposition (b, d and f) using mono- and bimetallic oxidized NPs (0.2 wt%) supported on D3 under simulated sunlight irradiation at pH 4.5 (a, b), pH 5 (c, d) and pH 6 (e, f). Legend: $Fe_{20}Cu_{80}$/D3 (○), $Fe_{80}Cu_{20}$/D3 (●), Fe_{ox}/D3 (□), Cu_{ox}/D3 (■), $Fe_{50}Cu_{50}$/D3 (◊). Reaction conditions: catalyst (~200 mg/L, 0.0071

mM supported Cu and/or Fe), phenol (100 mg L^{-1}, 1.06 mM), H_2O_2 (200 mg L^{-1}; 5.88 mM), 20 ºC, simulated sunlight (1 sun).

The photocatalytic activity of the most active $Fe_{20}Cu_{80}$(0.2 wt%)/D3 sample was also checked under natural sunlight irradiation as a function of the pH up to quasi-neutral pH values and compared with the performance of simulated sunlight (Figure 5). Similarly to the experiments using simulated sunlight irradiation, using natural sunlight the catalytic activity of $Fe_{20}Cu_{80}$(0.2 wt%)/D3 at pH 4 and 6 was again higher than that of the monometallic Fe_{ox}(0.2 wt%)/D3 or Cu_{ox}(0.2 wt%)/D3 (Figure S34).

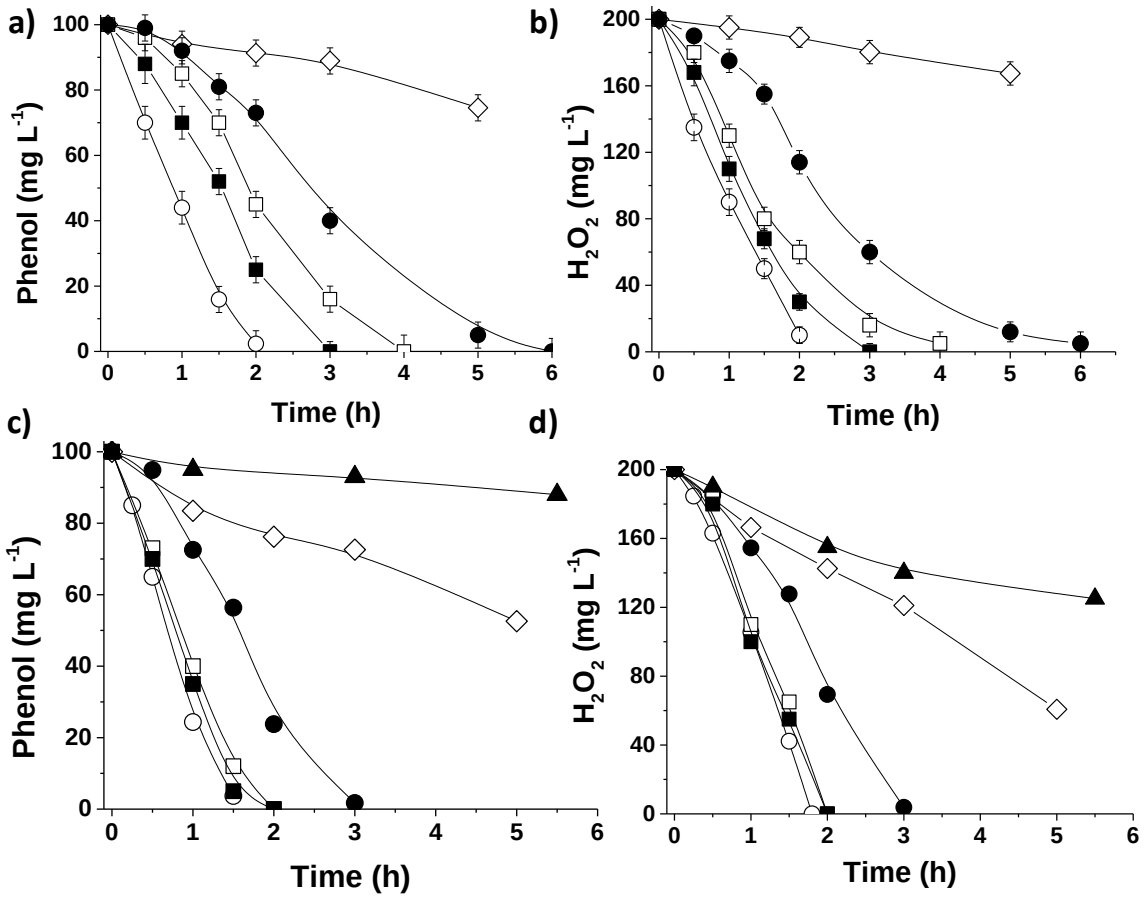

Figure 5. Phenol degradation (a, c) and H_2O_2 decomposition (b, d) as a function of the pH using simulated (a, b) or natural (c, d) sunlight irradiation using $Fe_{20}Cu_{80}$(0.2 wt%)/D3 as catalyst. Legend: pH 4 (○), pH 4.5 (■), pH 5 (□), pH 6 (●), pH 7 (◊) and pH 8 (▲). Reaction

conditions: catalyst (~200 mg/L, 0.0071 mM supported Cu and/or Fe), phenol (100 mg L^{-1}, 1.06 mM), H_2O_2 (200 mg L^{-1}; 5.88 mM), pH as indicated**,** simulated sunlight (1 sun, 20 ºC) or natural sunlight irradiation (980 mW cm^{-2} and 29 ºC). Irradiations with natural sunlight were performed the same day, to minimize unavoidable light intensity fluctuations.

The influence of the H_2O_2 to phenol molar ratio on the phenol degradation and on the concentration of its toxic reaction intermediates, hydroquinone, catechol and *p*-benzoquinone was also studied under optimal conditions. The results are presented in Figure S35. An optimum of 6.0 equivalents of H_2O_2 respect to phenol allows complete phenol disappearance. The resulting effluent after the photoFenton reaction with $Fe_{20}Cu_{80}$(0.2 wt%)/D3 was further treated by an aerobic biological process to check its biodegradability and the lack of ecotoxicity (absence of hydroquinone, catechol and *p*-benzoquinone). It was considered biodegradable when the BOD_5/COD ratio is higher than 0.4.. In good agreement with the biodegradability values under optimal reaction conditions (BOD_5/COD>0.4), the phenol mineralization based on TOC measurements at pH 4 and 6.0 equivalents of H_2O_2 resulted to be around 90 % of the carbon atoms of phenol being mineralized to CO_2. As expected, further increase of the H_2O_2 concentration to 6.5 or 7.5 equivalents resulted in a further increase of effluent biodegradability.

3.3. Catalyst stability

In order to assess the stability of the most active catalyst prepared in this work ($Fe_{20}Cu_{80}$/D3 at 0.2 wt% metal loading), several reuse experiments as well as measurements of possible leached metals from the solid catalyst to the reaction medium were performed at two pH values of 4 and 6 under simulated sunlight irradiation. Figure 6 shows that $Fe_{20}Cu_{80}$(0.2 wt%)/D3 catalyst can be reused up to five times with only slight decrease of its catalytic activity at both pH values. It should be noted that analogous Cu_{ox}(0.2 wt%)/D3

catalyst under similar reaction conditions undergoes immediate deactivation after one use, probably due to the complete oxidation of copper NPs to Cu^{2+}. The increased $Fe_{20}Cu_{80}$(0.2 wt%)/D3 catalyst stability respect to Cu_{ox}(0.2 wt%)/D3 exemplifies how it is possible to increase catalyst stability, in this case for the heterogeneous (photo)Fenton reaction, by preparing bimetallic NPs with adequate metals in optimal proportions. The five- and seven-times used catalyst at pH 4 and 6, respectively, were characterized by TEM (Figures S36 and Figure 7). A certain aggregation of the MNPs respect to the fresh sample (4.1 ± 0.77 nm) (Figure 1) was observed at pH 4 (5.1 ± 0.70 nm), but in much lesser extent at pH 6 (4.3± 0.70 nm) (Figure 7a). Analysis of the liquid phase after one catalytic cycle at pH 4 reveals the presence of iron (3μg L^{-1}) and copper (9 μg L^{-1}) species, but in lesser extent when working at pH 6 (1 and 3 μg L^{-1} for iron and copper, respectively). The metal leached away at pH 4 and 6 represents a percentage of about 3 and 1 wt%, respectively, of the initial metal content present in the fresh catalyst. Almost similar iron and copper leaching using the $Fe_{20}Cu_{80}$/D3 at pH 4 and 6 after five and seven uses were also found. The higher stability of $Fe_{20}Cu_{80}$(0.2 wt%)/D3 at pH 6 compared to that of pH 4 is in agreement with the fact that metals dissolve better in acidic conditions. At this point it is important to remind that the amounts of leached iron or copper are much lower than those concentrations permitted in some European Union countries, with the values for iron and copper of 0.2 and 2 mg L^{-1}, respectively [24].

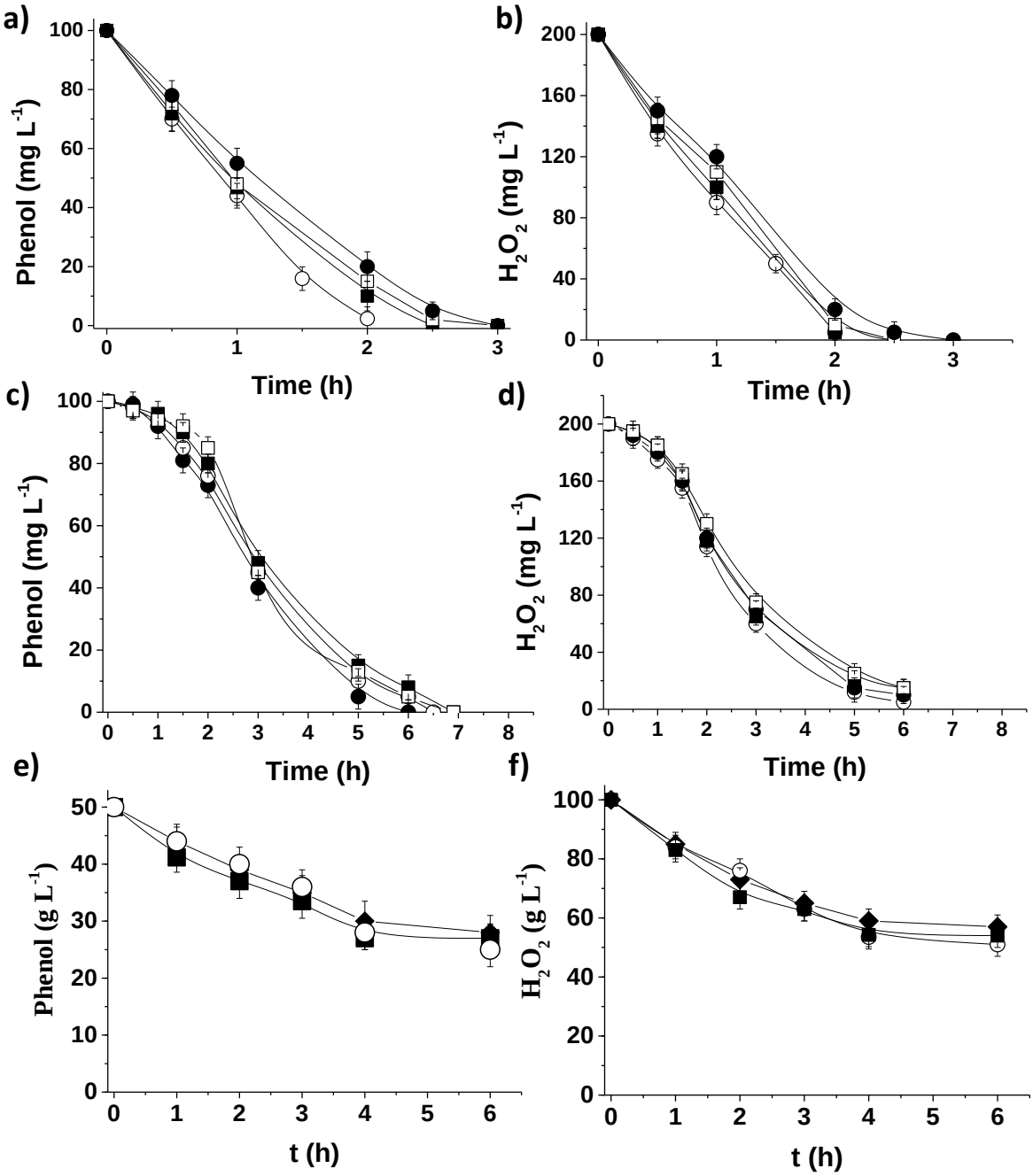

Figure 6. $Fe_{20}Cu_{80}$(0.2 wt%)/D3 **c**atalyst reusability for phenol degradation (a, c, e) and H_2O_2 decomposition (b, d, f) under different reaction conditions. (a, b) Reusability at pH 4. 1st use (○), 2nd use (■), 3th (□) use and 4th use (●). (c, d) Reusability at pH 6. 1st use (●), 3nd use (○), 5th (■) use and 7th use (□). (e, f) Reusability at pH 4 under productivity reaction conditions. 1st use (■), 2nd use (♦) and 3th (○) use. Legend: Reaction conditions for a-d: catalyst (~200 mg/L, 0.0071 mM supported Cu and/or Fe), phenol (100 mg L^{-1}, 1.06 mM), H_2O_2 (200 mg L^{-}

[1]; 5.88 mM), 20 ºC, pH 4 (a,b) and pH 6 (c,d), simulated sunlight (1 sun). Reaction conditions for e-f: Catalyst (200 mg/L, 0.2 wt% metal loading), phenol (50 g L^{-1}), H_2O_2 (100 g L^{-1}), pH 4, simulated sunlight irradiation.

In order to address the heterogeneity of the reaction, a control experiment at pH 4 under simulated sunlight irradiation was carried out in the absence of any solid catalyst but adding 3 wt% of soluble salts of iron and copper respect to the metal content in the fresh $Fe_{20}Cu_{80}$(0.2 wt%)/D3 catalyst (Figure S37). It was observed that phenol conversion of this homogeneous phase (photo)Fenton reaction is lower than 20 %, while, in contrast, the conversion in the presence of the heterogeneous catalysts under these conditions at this reaction time is 100 % (Figure S37). Even more, another homogeneous phase control under similar reaction conditions using the same amount of iron and copper than the total amount present in the heterogeneous catalyst results in a conversion of only 44 % at 2 h working at pH 4 (Figure S37). Similarly, another homogeneous phase experiment using the total amount of metal present in the heterogeneous catalyst at pH 6 resulted in a conversion at 3 h lower (70 %) respect to that of the heterogeneous catalyst (100 %). These control experiments reflect the benefits of an adequate proportion of bimetallic FeCu NP supported on D3 as heterogeneous catalyst under visible light irradiation.

In summary, the TEM and leaching measurements evidence the higher stability of the $Fe_{20}Cu_{80}$(0.2 wt%)/D3 catalyst at pH 6 respect to 4 and, therefore, its better reusability. In this context, the EPR spectra of the seven-times used catalyst at pH 6 show a slight increase of its intensity that may be attributed to the increase of paramagnetic species such as Fe^{3+} and/or Cu^{2+} respect to the fresh catalyst (Figure 7b). In a previous work, a higher EPR intensity was observed for Cu_{ox}(0.2 wt%)/D3 catalyst after its use in the heterogeneous (photo)Fenton reaction and attributed to the oxidation of the EPR silent reduced Cu^0/Cu^+ species to catalytically less active Cu^{2+} causing catalyst deactivation [17]. In the present case,

the $Fe_{20}Cu_{80}$(0.2 wt%)/D3 shows a good stability and reusability, especially at pH 6, showing the benefits of the mixed oxide as multiredox centre able to maintain the copper species in the catalyst in their low oxidation state as it will be discussed below.

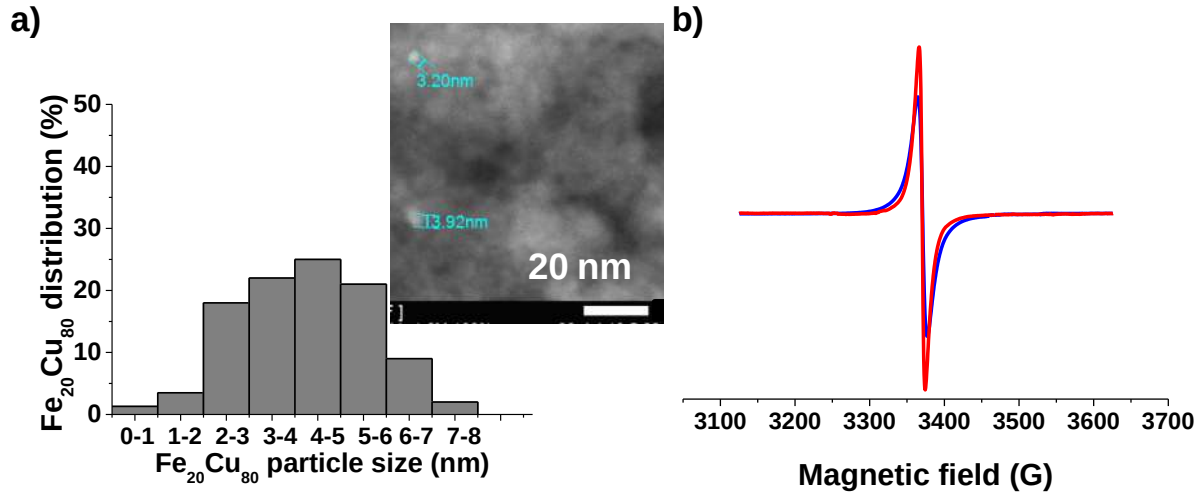

Figure 7. Particle size distribution and DF-STEM image of $Fe_{20}Cu_{80}$(0.2 wt%)/D3 used seven-times as photocatalyst at pH 6: b) EPR spectra of the fresh (blue line) and seven-times used (red line) $Fe_{20}Cu_{80}$/D3 catalyst.

In order to compare the photocatalytic activity of $Fe_{20}Cu_{80}$(0.2 wt%)/D3 with that of other related materials previously reported, a productivity test using a large amount of phenol and H_2O_2 respect to the $Fe_{20}Cu_{80}$/D3 catalyst at pH 4 under simulated sunlight irradiation was performed. This productivity test allows estimating after three consecutive uses an accumulated TON of about 105,000 (Figure 6 e-f). This TON value is higher than that obtained using the analogous catalyst Fe_{ox}(0.2 wt%)/D3 catalyst (TON 38,000) [18] or Cu_{ox}(0.2 wt%)/D3 (TON 52,000) [17]. Interestingly, in other experiment working with the $Fe_{20}Cu_{80}$(0.2 wt%)/D3 catalyst at pH 6 under natural sunlight irradiation a TON in a single catalytic cycle of 6,700 was achieved (Figure S38). This is one of the few existing examples reported in the literature with such a high TON at quasi neutral pH with a low excess of H_2O_2 (6.0 equivalents) under natural sunlight irradiation.

It should be commented that typically Fenton reactions at quasi neutral pH are carried out with 10,000 equivalents or higher of H_2O_2 and the present reaction conditions are substantially more attractive economically than those of previous reports [25].

3.4. Transient absorption spectroscopy and EPR study

In order to get some insights about the reaction mechanism in the presence of $Fe_{20}Cu_{80}$(0.2 wt%)/D3 photocatalyst, a transient absorption spectroscopy study was carried out. Supporting information provides a detailed description of the transient absorption spectroscopy measurements and the quenching studies (Section S8 and Figures S39-42). A transient absorption spectra of $Fe_{20}Cu_{80}$(0.2 wt%)/D3 in an acetonitrile suspension upon excitation at 532 nm was recorded and attributed to photo-generated electrons arising from photoinduced charge separation. This proposal was compatible with the quenching experiments by dichloromethane and methanol as electron donor and acceptor quencher, respectively.

Besides to transient absorption spectroscopy, selective quenching experiments and EPR spectroscopy were performed to characterize the reactive oxygen species involved in the photoFenton reaction using $Fe_{20}Cu_{80}$(0.2 wt%)/D3 as catalyst under visible light irradiation. As it can be seen in Figure S43, addition of DMSO, a well-known hydroxyl radical scavenger [26], to the photocatalytic system completely stops the phenol degradation, thus, providing evidence in support of the involvement of hydroxyl radicals. The formation of hydroxyl radicals was validated by EPR spectroscopy using 5,5-Dimethyl-1-pyrroline N-oxide (DMPO) as spin trap. The corresponding EPR spectra are provided in the supporting information (Figure S43).

3.5. Mixed oxide versus single metal oxide

Based on the above catalytic and spectroscopic data as well as on the fundamentals of the Fenton chemistry using iron and/or copper species [3,22,27], the reaction mechanism

summarized in Scheme 1 is proposed. The key finding of the present study is the higher catalytic activity of $Fe_{20}Cu_{80}$(0.2 wt%)/D3 than that of Fe_{ox}(0.2 wt%)/D3 or Cu_{ox}(0.2 wt%)/D3, even though the last two samples have smaller metal particle size. In order to clarify the reasons of the higher activity of the mixed metal oxide, in the present work we should consider not only the particle size distribution, but also the metal NP composition and the reactivity with H_2O_2. Scheme 1 shows some reported rate constants for Cu and Fe species. As it can be seen for the rate constant of Cu^+ reacting H_2O_2 to produce $HO^{\cdot}$ radicals is higher respect to Fe^{2+}. On the contrary, Cu^{2+} reduction by H_2O_2 is about 2600 times slower than the Fe^{3+} reduction to Fe^{2+}. These kinetic data for homogeneous phase agree with the efficiency of Cu_{ox}(0.2 wt%)/D3 for H_2O_2 reduction to $HO^{\cdot}$ radicals assisted by visible light irradiation. However, Cu_{ox}(0.2 wt%)/D3 deactivates fast due to the formation of Cu^{2+} species that is only slowly converted to Cu^+. In the case, of Fe_{ox}(0.2 wt%)/D3 the easier reduction of Fe^{3+} to Fe^{2+} by H_2O_2 respect to Cu^{2+} is the main reason for Fe_{ox}(0.2 wt%)/D3 good recyclability without significant deactivation. In this context, the increased activity of $Fe_{20}Cu_{80}$(0.2 wt%)/D3 in spite of its higher metal particle size respect to its counter parts Fe_{ox}(0.2 wt%)/D3 or Cu_{ox}(0.2 wt%)/D3 can be further understood considering that this sample combines the kinetically favorable rate for the formation of $HO^{\cdot}$ radicals due to Cu^+ with the good recyclability due to the presence of Fe^{3+} in appropriate proportion. Thus, the high activity and stability of $Fe_{20}Cu_{80}$(0.2 wt%)/D3 suggest that in this catalyst Fe^{2+} is able to reduce Cu^{2+} again to Cu^+ recovering the catalytic activity. Subsequently Fe^{3+} will be easily reduced to Fe^{2+} either photocatalytically or by H_2O_2. Thus, the combination of the two metals renders active and stable active sites.

Dark conditions

$Cu^{+} + H_2O_2 \rightarrow Cu^{2+} + HO^{\cdot} + HO^{-}$ $k = 1 \cdot 10^{4}\ M\ s^{-1}$

$Cu^{2+} + H_2O_2 \rightarrow Cu^{+} + HOO^{\cdot} + H^{+}$ $k = 1.15 \cdot 10^{-6}\ M\ s^{-1}$

$Fe^{2+} + H_2O_2 \rightarrow Fe^{3+} + HO^{\cdot} + HO^{-}$ $k = 76\ M\ s^{-1}$

$Fe^{3+} + H_2O_2 \rightarrow Fe^{2+} + HOO^{\cdot} + H^{+}$ $k = 0.003\ M^{-1}\ s^{-1}$

$Fe^{2+} + Cu^{2+} \rightarrow Fe^{3+} + Cu^{+}$ $\Delta E^{0} = 0.6\ eV$

Visible ligh irradiation

$Fe_{20}Cu_{80}/D_3 + h\nu \rightarrow e^{-} + h^{+}$

$H_2O_2 + e^{-} \rightarrow HO^{\cdot} + HO^{-}$

$Fe^{3+} + e^{-} \rightarrow Fe^{2+}$

$Cu^{2+} + e^{-} \rightarrow Cu^{+}$

$Cu^{+} + e^{-} \rightarrow Cu^{0}$

$h^{+} + H_2O_2 \rightarrow HOO^{\cdot} + H^{+}$

$h^{+} + Fe^{2+} \rightarrow Fe^{3+}$

$h^{+} + Cu^{+} \rightarrow Cu^{2+}$

h^{+} + organic compunds → oxidized products

Scheme 1. Mechanistic proposal for the photoFenton reaction promoted by $Fe_{20}Cu_{80}$(0.2 wt%)/D3 explaining higher activity respect to Fe_{ox}(0.2 wt%)/D3 and higher stability respect to Cu_{ox}(0.2 wt%)/D3, due to the operation of Fe^{2+} reduction of Cu^{2+}.

Moreover, as it has been shown the catalytic activity of $Fe_{20}Cu_{80}$(0.2 wt%)/D3 for H_2O_2 activation is substantially enhanced by sunlight irradiation. Based on transient absorption spectroscopy, visible light irradiation of $Fe_{20}Cu_{80}$/D3 sample at 532 nm leads to the photogeneration of electrons and holes. According Scheme 1, these electrons can promote the one-electron reduction of H_2O_2 to $HO^{\cdot}$ radicals as evidenced by EPR measurements, while reduced iron or copper species can be reoxidized achieving a stationary distribution of metal ions in various oxidation states that are suitable for optimal photocatalytic activity. In

agreement with previous reports, here it is also proposed that the role of D3 is to anchor well-dispersed $Fe_{20}Cu_{80}$ NPs, maintaining their small particle size, and allowing the diffusion of hydroxyl radicals to the aqueous phase due to the inertness of the diamond surface.

Conclusions

Preparation of an optimized catalyst based on bimetallic oxide NPs namely $Fe_{20}Cu_{80}$(0.2 wt%)/D3 has been achieved. The hydroxylated surface of nanometric diamond allows the formation of small Fe-Cu NP (4.1 ± 0.77 nm) at 0.2 wt% metal loading. The resulting heterogeneous catalyst having abundant transition metals is highly active and reusable catalyst at pH 6 for the heterogeneous Fenton reaction assisted by natural or simulated sunlight irradiation achieving a mineralization degree of 90 % at a H_2O_2 to phenol molar ratio of 6. The higher activity of $Fe_{20}Cu_{80}$(0.2 wt%)/D3 respect to analogous catalysts based on graphite or activated carbon can be attributed to the smaller metal particle size and the inertness of the diamond surface. The activity of $Fe_{20}Cu_{80}$(0.2 wt%)/D3 resulted to be higher than that of the benchmark $Fe_{20}Cu_{80}$(0.2 wt%)/TiO_2-P25 reference material that partially decomposes H_2O_2 spuriously to O_2 without effecting the phenol degradation. Based on the catalytic data, transient absorption spectroscopy, EPR spectroscopy measurements and the well-known Fenton chemistry of iron and copper species, the two main reasons of the high activity and stability of $Fe_{20}Cu_{80}$(0.2 wt%)/D3 catalyst under visible light appear to be the high activity of reduced copper to form hydroxyl radicals and the favorable redox process of Fe^{2+} maintaining a pool of reduced Cu^{+} species.

Overall the present study has shown the possibility to develop stable heterogeneous catalysts based on abundant iron or copper metals to promote the H_2O_2 activation to hydroxyl radicals under visible light irradiation.

References

[1] S. Malato, P. Fernández-Ibáñez, M.I. Maldonado, J. Blanco, W. Gernjak, Decontamination and disinfection of water by solar photocatalysis: Recent overview and trends, Cat. Today 147 (2009) 1-59.

[2] M. Pera-Titus, V. García-Molina, M.A. Baños, J. Giménez, S. Esplugas, Degradation of chlorophenols by means of advanced oxidation processes: a general review Appl. Catal. B-Environ. 47 (2004) 219-256.

[3] J.J. Pignatello, E. Oliveros, A. MacKay, Advanced oxidation processes for organic contaminant destruction based on the fenton reaction and related chemistry Crit. Rev. Env. Sci. Tec. 36 (2006) 1-84.

[4] S.R. Pouran, A.R.A. Aziz, V.M.A.W. Daud, Review on the main advances in photo-Fenton oxidation system for recalcitrant wastewaters, J. Ind. Eng. Chem. 21 (2015) 53-69.

[5] M. Cheng, G. Zeng, D. Huang, C. Lai, P. Xu, C. Zhang, Y. Liu, Hydroxyl radicals based advanced oxidation processes (AOPs) for remediation of soils contaminated with organic compounds: A review Chem. Eng. J. 298 (2016) 582-598.

[6] E.G. Garrido-Ramírez, B.K.G. Theng, M.L. Mora, Clays and oxide minerals as catalysts and nanocatalysts in Fenton-like reactions - A review, Appl. Clay Sci. 47 (2010) 182-192.

[7] M. Klavarioti, D. Mantzavinos, D. Kassinos, Removal of residual pharmaceuticals from aqueous systems by advanced oxidation processes, Env. Int. 35 (2009) 402-417.

[8] E. Morillo, J. Villaverde, Advanced technologies for the remediation of pesticide-contaminated soils, Sci. Total Environ. (2017) 576-597

[9] A.D. Bokare, W. Choi, Review of iron-free Fenton-like systems for activating H2O2 in advanced oxidation processes J. Hazard. Mater. 275 (2014) 121-135.

[10] S. Chiron, A. Fernandez-Alba, A. Rodriguez, E. Garcia-Calvo, Pesticide chemical oxidation: State-of-the-art, Water Res. 34 (2000) 366-377.

[11] M.N. Chong, B. Jin, C.W.K. Chow, C. Saint, Recent developments in photocatalytic water treatment technology: A review, Water Res. 44 (2010) 2997-3027.

[12] J. Herney-Ramirez, Vicente, M.A., Madeira, L.M., Heterogeneous photo-Fenton oxidation with pillared clay-based catalysts for wastewater treatment: A review, Appl. Catal. B-Environ. 98 (2010) 10-26.

[13] C. Wang, H. Liu, Z. Sun, Heterogeneous photo-Fenton reaction catalyzed by nanosized iron oxides for water treatment Int. J. Photoenergy (2012) 801694.

[14] J.H. Ramírez, F.J. Maldonado-Hódar, A.F. Perez-Cadenas, C. Moreno-Castillo, C.A. Costa, L.A. Madeira, Azo-dye Orange II degradation by heterogeneous Fenton-like reaction using carbon-Fe catalysts, Appl. Catal. B: Environ. 75 (2007) 312-323.

[15] S. Navalon, D. Sempere, M. Alvaro, H. Garcia, Influence of hydrogen annealing on the photocatalytic activity of diamond-supported gold catalysts, ACS Appl. Mater. Interfaces 5 (2013) 7160-7169.

[16] J.C. Espinosa, S. Navalón, M. Álvaro, H. García, Silver nanoparticles supported on diamond nanoparticles as a highly efficient photocatalyst for the Fenton reaction under natural sunlight irradiation, ChemCatChem 7 (2015) 2682-2688.

[17] J.C. Espinosa, S. Navalón, M. Álvaro, H. García, Copper nanoparticles supported on diamond nanoparticles as a cost-effective and efficient catalyst for natural sunlight assisted Fenton reaction, Catal. Sci. Technol. 6 (2016) 7077-7085.

[18] J.C. Espinosa, C. Catalá, S. Navalón, B. Ferrer, M. Álvaro, H. García, Iron oxide nanoparticles supported on diamond nanoparticles as efficient and stable catalyst for the visible light assisted Fenton reaction, Appl. Catal. B. Environ. 226 (2018) 242-251

[19] P.A. Morozov, B.G. Ershov, The influence of phosphates on the decomposition of ozone in water: chain process inhibition, Russ. J. Phys. Chem. 84 (2010) 1136-1140.

[20] M. Mehrvar, W.A. Anderson, M. Moo-Young, Photocatalytic degradation of aqueous organic solvents in the presence of hydroxyl radical scavengers, Int. J. Photoenergy 3 (2002) 187-191.

[21] E.G. Garrido-Ramírez, J.F. Marco, N. Escalona, M.S. Ureta-Zañnartu, Preparation and characterization of bimetallic FeCu allophane nanoclays and their activity in the phenol oxidation by heterogeneous electro-Fenton reaction, Micropor. Mesopor. Mater. 225 (2016) 303-311.

[22] S. Karthikeyan, M.P. Pachamuthu, M.A. Isaacs, S. Kumar, A.F. Lee, G. Sekaran, Cu and Fe oxides dispersed on SBA-15: A Fenton type bimetalliccatalyst for N,N-diethyl-p-phenyl diamine degradation, Appl. Catal. B. Environ. 199 (2016) 323-330.

[23] R. Martin, Navalon, S., Delgado, J.J., Calvino, J.J., Alvaro, M., Garcia, H., Influence of the preparation procedure on the catalytic activity of gold supported on diamond nanoparticles for phenol peroxidation, Chem. Eur. J. 17 (2011) 9494-9502.

[24] Council Directive 98/83/EC of 3 November 1998 on the quality of water intended for human consumption.

[25] A. Dhakshinamoorthy, S. Navalon, M. Alvaro, H. Garcia, Metal nanoparticles as heterogeneous fenton catalyst, ChemSusChem 5 (2012) 46-64.

[26] M.J. Burkitt, R.P. Mason, Direct evidence for in vivo hydroxyl-radical generation in experimental iron overload: An ESR spin-trapping investigation Proc. Natl. Acad. Sci. USA 88 (1991) 8440-8444.

[27] K. Li, Y. Zhao, M.J. Janik, C. Song, X. Guo, Facile preparation of magnetic mesoporous Fe3O4/C/Cu composites as high performance Fenton-like catalysts, App. Surf. Sci. 396 (2017) 1383-1392.

Acknowledgements

S.N. thanks financial support by the Fundación Ramón Areces (XVIII Concurso Nacional para la Adjudicación de Ayudas a la Investigación en Ciencias de la Vida y de la Materia, 2016), Ministerio de Ciencia, Innovación y Universidades RTI2018-099482-A-I00 project and Generalitat Valenciana grupos de investigación consolidables 2019 (ref: AICO/2019/214) project. H.G. thanks financial support by the Spanish Ministry of Science and Innovation (Severo Ochoa SEV2016 and RTI2018-890237-CO2-1) and Generalitat Valenciana (Prometeo 2017/083) is also gratefully acknowledged.